



Network-based statistics distinguish anomic and Broca's aphasia

Nicholas Riccardi¹ · Xingpei Zhao² · Dirk-Bart den Ouden³ · Julius Fridriksson³ · Rutvik H. Desai¹ · Yuan Wang²

Received: 3 March 2023 / Accepted: 21 November 2023

© The Author(s), under exclusive licence to Springer-Verlag GmbH Germany, part of Springer Nature 2023

Abstract

Introduction Aphasia is a speech-language impairment commonly caused by damage to the left hemisphere. The neural mechanisms that underpin different types of aphasia and their symptoms are still not fully understood. This study aims to identify differences in resting-state functional connectivity between anomic and Broca's aphasia measured through resting-state functional magnetic resonance imaging (rs-fMRI).

Methods We used the network-based statistic (NBS) method, as well as voxel- and connectome-based lesion symptom mapping (V-, CLSM), to identify distinct neural correlates of the anomic and Broca's groups. To control for lesion effect, we included lesion volume as a covariate in both the NBS method and LSM.

Results NBS identified a subnetwork located in the dorsal language stream bilaterally, including supramarginal gyrus, primary sensory, motor, and auditory cortices, and insula. The connections in the subnetwork were weaker in the Broca's group than the anomic group. The properties of the subnetwork were examined through complex network measures, which indicated that regions in right inferior frontal sulcus, right paracentral lobule, and bilateral superior temporal gyrus exhibit intensive interaction. Left superior temporal gyrus, right postcentral gyrus, and left supramarginal gyrus play an important role in information flow and overall communication efficiency. Disruption of this network underlies the constellation of symptoms associated with Broca's aphasia. Whole-brain CLSM did not detect any significant connections, suggesting an advantage of NBS when thousands of connections are considered. However, CLSM identified connections that differentiated Broca's from anomic aphasia when analysis was restricted to a hypothesized network of interest.

Discussion We identified novel signatures of resting-state brain network differences between groups of individuals with anomic and Broca's aphasia. We identified a subnetwork of connections that statistically differentiated the resting-state brain networks of the two groups, in comparison with standard CLSM results that yielded isolated connections. Network-level analyses are useful tools for the investigation of the neural correlates of language deficits post-stroke.

Keywords Aphasia · fMRI · Brain network model · Lesion symptom mapping

Introduction

Aphasia is a speech-language disorder that commonly develops after a left-hemisphere stroke and can affect a person's ability to read, understand, and speak a language.

Nicholas Riccardi and Xingpei Zhao—Equal contributions.

✉ Yuan Wang
wang578@mailbox.sc.edu

¹ Department of Psychology, University of South Carolina, Columbia, SC, USA

² Department of Epidemiology and Biostatistics, University of South Carolina, Columbia, SC, USA

³ Department of Communication Sciences and Disorders, University of South Carolina, Columbia, SC, USA

According to the National Aphasia Association, aphasia currently affects over 2 million Americans. There are several types of aphasia based on individual behavioral symptoms. Classification of aphasia types remains controversial, and can depend on differences between raters or the specific diagnostic tests used (Wertz et al. 1984). Individuals with different types of aphasia often exhibit overlapping sets of symptoms, while those within the same type can differ significantly (Casilio et al. 2019). Nonetheless, patterns of symptoms associated with aphasia types can be observed when measured by well-validated diagnostic materials such as the Western Aphasia Battery (Kertesz 2007). Prior research has demonstrated that aphasia types can be used to effectively investigate the neurobiology of language, providing insights on how patterns of brain damage (or residual

brain health) can be associated with constellations of symptoms (Yourganov et al. 2015a; Robson et al. 2014; Fridriksson et al. 2015). Examining the neural correlates of aphasia syndromes has been a goal of neuroscience for over a century (Broca 1861), and remains a topic of high scientific and clinical importance (Fridriksson et al. 2018; Desai and Riccardi 2021).

Two common types of post-stroke aphasia that are primarily characterized by speech production problems, as opposed to comprehension problems, are anomic and Broca's aphasia. Anomic aphasia is a fluent type of aphasia characterized by problems with word retrieval. Individuals with anomic aphasia may block upon failing word retrieval, or use circumlocution, but their speech fluency, repetition, comprehension, and grammatical speech are relatively preserved (Dronkers and Baldo 2009). On the other hand, Broca's aphasia is a non-fluent type of aphasia that may exhibit agrammatic speech output and poor repetition (Hickok 2009). Their comprehension of spoken and written language often remains intact or has relatively mild impairments. As difficulty with word retrieval is related to damage throughout much of the peri-Sylvian region (Dronkers and Baldo 2009), word finding difficulties can be observed in both anomic and Broca's aphasia (Whitaker 2007). However, the severity level and performance patterns are different in the two types of aphasia. For instance, it has been reported to be more difficult for individuals with anomic aphasia to retrieve nouns and for individuals with Broca's aphasia to retrieve verbs (Miceli et al. 1988; Zingeser and Berndt 1990). Behaviorally and diagnostically, the primary difference between speakers with Broca's aphasia and anomic aphasia is the typically reduced speech fluency and repetition performance in Broca's aphasia (Kertesz 2007). In addition, Broca's aphasia often co-occurs with expressive agrammatism, in the form of reduced sentence complexity and problems with morpho-syntactic markers, such as inflections and function words, in production (Friedmann 2009; Goodglass et al. 2001; Hillis 2007). It must be noted, however, that neither the articulatory deficit nor the agrammatism are essential diagnostic features of the Broca's aphasia syndrome.

In terms of neural mechanisms, the left inferior frontal regions, especially pars triangularis and pars opercularis traditionally referred to as 'Broca's area' (although see (Tremblay and Dick 2016) regarding terminology), have traditionally been associated with syntactic processing in language production and comprehension (Caramazza and Berndt 1978; Keller et al. 2009). The impairment to Broca's area alone, however, does not explain impaired syntactic comprehension and production in Broca's aphasia (Mohr et al. 1978). Grammatical impairments are associated with damage to a larger area surrounding Broca's area or other different brain area, such as lateral portion of the anterior temporal lobe (Dronkers and Baldo 2009) and even posterior temporal

cortex (Den Ouden et al. 2019). One hypothesis is that the impairment in a collection of speech-language functions in post-stroke Broca's aphasia is related to the damage to brain regions supplied by the superior division of the left middle cerebral artery (Dronkers and Baldo 2009; Hillis 2007; Dronkers et al. 2004; Zaidel et al. 1995). Besides, grammatical and sentence-level language processing is a higher-level language function and requires a series of complex mechanisms to process multiple information sources (Caplan et al. 2000; Fiebach and Schubotz 2006; Matchin and Hickok 2020). As such, dysfunction within intrinsic brain networks may explain the agrammatic speech and difficulties in comprehension of complex sentences often observed in Broca's aphasia (Zhu et al. 2014; Tomasi and Volkow 2012). On the other hand, the object-naming difficulty in anomic aphasia cannot typically be attributed to damage in specific brain regions (Yourganov et al. 2015b; Fridriksson et al. 2018). In sum, the neural mechanisms associated with anomic and Broca's aphasia are not fully understood, especially pertaining to possible interactions between partially damaged or spared brain areas at a network-level. Connectome-based analyses that examine structural or functional connectivity between brain regions are useful methods in this context, and other studies have shown that they provide information that is complementary to standard lesion overlap methods (Blackett et al. 2022; Gleichgerrcht et al. 2017a; Riccardi et al. 2022)

Functional magnetic resonance imaging (fMRI) (Ogawa et al. 1992; Rogers et al. 2001) is a neuroimaging technique for investigating functional brain activity through blood-oxygen-level-dependent (BOLD) fluctuations in different brain regions. Resting-state fMRI (rs-fMRI) is acquired in the absence of any tasks (Fox and Raichle 2007). Brain network models based on rs-fMRI describe intrinsic coherent functional activity in a resting brain and are considered to be permanent, trait-like functional signatures (Hjelmervik et al. 2014). Network models can be applied to examine inter-relationships of these fluctuations in regions of interest (ROIs). In a brain network built on ROI-segmented fMRI data, the ROIs serve as nodes and functional connections between the ROIs serve as edges. The strength of functional connections is typically measured by correlation between the BOLD signals of two regions. Using such a connectome provides some advantages over standard lesion overlap methods (Gleichgerrcht et al. 2017a). First, an rs-fMRI connectome uses information from both necrotic and spared tissue, while lesion overlap methods can only make inferences from areas of necrosis. In an rs-fMRI connectome, damaged areas will have low connectivity to other regions, while healthy areas will have a wider range of connectivity profiles that can reflect intrinsic activity or post-stroke reorganization (Wilson and Schneck 2020). This allows for brain-behavior inferences about areas outside of the stroke territory, such as

the spared contralateral hemisphere (Yourganov et al. 2021; Riccardi et al. 2020). Second, due to diaschisis (Carrera and Tononi 2014), disrupted connectivity between two areas (A and B), can be caused by damage to area C. Connectome measures can detect behavioral correlates of connectivity between areas A and B, while lesion overlap will attribute behavior only to area C. Finally, and relatedly, voxelwise lesion-symptom mapping requires a high degree of necrotic overlap at the millimeter level to detect effects, while the connectome can detect levels of (dis)connectivity between areas A and B across multiple participants who may have very different patterns of necrosis (Gleichgerricht et al. 2017a).

Studies comparing resting-state networks from stroke-survivors with aphasia and healthy controls have revealed that the peri-Sylvian region, posterior middle temporal gyrus, anterior superior temporal gyrus, superior temporal sulcus, and Brodmann's area 47 of the inferior frontal gyrus in the left hemisphere are involved in semantic processing and language comprehension (Dronkers et al. 2004; Turken and Dronkers 2011; Zhu et al. 2014). These studies suggest that rs-fMRI is relevant in understanding network-level brain dysfunctions in people with aphasia. Their approaches focused on functional connectivity among selected ROIs in the left hemisphere. However, according to Yang et al. (2016, 2017), intrinsic regional brain dysfunctions in aphasia are associated with functional connectivity patterns in regions across the brain. Consequently, it is essential to investigate whole-brain functional connectivity in aphasia. So far, only a few studies have assessed resting-state whole-brain functional connectivity (Yang et al. 2016; Siegel et al. 2016; Guo et al. 2019; Yang et al. 2017). Siegel et al. (2016) predicted impairment in multiple behavioral domains based on associated resting-state functional connectivity and lesion location via machine-learning models. Yang et al. (2017) used multivariate pattern analysis to identify whole-brain functional connectivity patterns that distinguish stroke survivors with aphasia and healthy controls. To the best of our knowledge, no study has directly compared resting-state whole-brain functional connectivity between speakers with anomic versus Broca's aphasia. Such an analysis could provide novel information about the neural organization of language by detecting functional connections in healthy and necrotic areas that are associated with a given constellation of symptoms.

To identify distinct functional connections between two groups, a standard approach is to examine differences at each connection through mass univariate testing, where a large number of hypothesis tests are typically performed. After rs-fMRI data are preprocessed with an atlas, the number of ROIs can exceed 300. For instance, 384 ROIs are created by the atlas of intrinsic connectivity of homotopic areas (AICHA) (Joliot et al. 2015), yielding more than 70,000 connections between the ROIs. With such a large number

of hypothesis tests, the adjusted p -values after standard multiple comparison correction are large and may fail to detect significant differences in connections. Thus, the mass univariate testing approach may provide insufficient power, especially when distinct connections are not independent. A multivariate approach may aid with sensitivity for detection of non-independent connections. However, multivariate lesion-symptom mapping (LSM) may provide misleading results if not trained on data from hundreds (or even thousands) of participants Sperber et al. (2019); Mah et al. (2014), and much prior work has already been done to directly compare multivariate to univariate LSM, revealing that the two methods often provide equivalent results (Sperber et al. 2019; Karnath et al. 2018; Ivanova et al. 2021). In cases where data from hundreds of participants are not available to train a reliable multivariate model, univariate methods are recommended.

The network-based statistic (NBS) method (Zalesky et al. 2010) is a graph-theoretic approach that provides an efficient process to identify a subnetwork that distinguishes two groups of brain networks. The NBS method offers a substantial gain in power when such a subnetwork exists. From the comparisons of networks between healthy controls and participants with schizophrenia (Zalesky et al. 2010), Alzheimer's Disease (Zhan et al. 2016), internet addiction (Wen and Hsieh 2016), and borderline personality disorder (Xu et al. 2016), the NBS method has identified one or more altered subnetworks related to these neurological or psychiatric disorders. Furthermore, we can assess the network properties of the subnetwork by complex network measures (Rubinov and Sporns 2010). In this study, we apply the NBS method for the first time to rs-fMRI data of individuals with anomic and Broca's aphasia. We aim to identify rs-fMRI subnetworks that distinguish anomic and Broca's aphasia, thereby providing information about the neuroanatomical correlates of two commonly diagnosed aphasia syndromes. We also compare NBS findings with standard voxel- and connectivity-based LSM in order to demonstrate some differences between the methods.

Methods

Study description

Participants were recruited by the Center for the Study of Aphasia Recovery (C-STAR), to investigate language outcomes post-stroke. Only participants with a single ischemic or a hemorrhagic stroke in the left hemisphere were included. The participants with lacunar infarcts or with isolated damage in brainstem or cerebellum were excluded. The research was approved by the Institutional Review Board

(IRB) at the University of South Carolina and Medical University of South Carolina.

Participants

Aphasia types were classified based on the Western Aphasia Battery-Revised (WAB-R) (Kertesz 2007), which was administered by licensed speech-language pathologists (for full details of data fidelity and quality control, see (Spell et al. 2020)). Among the 96 participants included in the study sample, 39 were diagnosed with anomic aphasia, and 57 were diagnosed with Broca's aphasia. Figure 1 shows a lesion overlap map of the participants in the two groups. Demographic statistics of the two groups are summarized in Table 1. The mean age in the anomic group was 62.73 y.o. (s.d. = 11.97; range = 41) and the mean age in the Broca's group is 59.82 y.o. (s.d. = 10.35; range = 39). Respectively 60% and 68% of the participants in the anomic and Broca's group were male. There was no significant difference in age and gender between the anomic and Broca's group (age: p -value = 0.42 by two-sample t -test; gender: p = 0.74 by χ^2

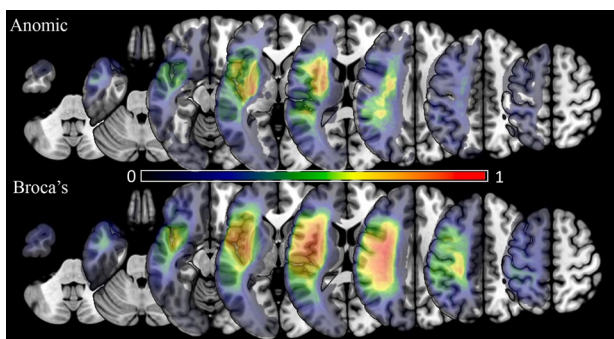


Fig. 1 Overlap of lesions across patients of anomic and Broca's aphasia. A voxel with overlap = 1 indicates that this voxel is lesioned in all patients in that group

-test). All participants were in the chronic (>6 months) stage of stroke, where brain and behavior are more stable than in the initial months following stroke (acute stage) (Maas et al. 2012). For the anomic group, time post-stroke was a mean of 2.9 y (s.d. = 3.42; range = 15) and for Broca's was 4.3 y (s.d. = 4.29; range = 16.5). This difference was not significant ($p > .1$). The mean WAB-R score for the anomic group was 85.74 (s.d. = 6.38; range = 22.1) and 46.44 (s.d. = 16.93; range = 59.1) for the Broca's group. As shown in Fig. 2, the WAB-R score for the anomic group is significantly higher than the Broca's group (p -value < 0.01 by two-sample t -test), since the participants with Broca's aphasia tend to have a lower score in the section of fluency and repetition than the participants with anomic aphasia.

Data acquisition and preprocessing

The rs-fMRI data were acquired on a Siemens Prisma 3T scanner with a 20-channel head coil located at the Center for the Study of Aphasia Recovery at the University of South Carolina. The following imaging parameters of images were used: a multiband sequence ($\times 2$) with a 216×216 mm field of view, a 90×90 matrix size, and a 72-degree flip angle, 50 axial slices (2 mm thick with 20% gap yielding 2.4 mm between slice centers), repetition time TR = 1650 ms, TE = 35 ms, GRAPPA = 2, 44 reference lines, interleaved ascending slice order. During the scanning process, the participants were instructed to stay still with eyes closed. A total of 370 volumes were acquired.

The rs-fMRI data were corrected for motion using the Realign and Unwarp procedure in SPM12 with default settings. Brain extraction was then performed using the SPM12 script pm_brain_mask with default settings. Slice time correction was also done using SPM12. The mean fMRI volume for each participant was then aligned to the corresponding T2-weighted image to compute the spatial transformation between the data and the lesion mask. The fMRI data

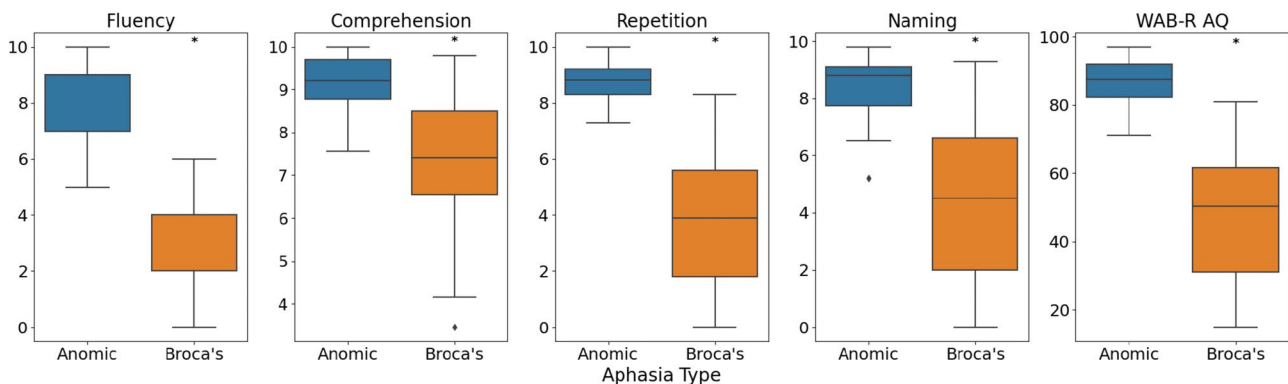


Fig. 2 Box plots of WAB-R and major subscores of the 96 participants. Asterisk denotes a significant difference between the groups (two-tailed t -test, $p < .05$)

Table 1 Demographic statistics of participants with anomic and Broca's aphasia: mean and standard deviation of age and WAB-R score, percentages of race/ethnicity and education levels out of all participants in the study. (*Two-sample *t*-test was used to test group difference in age, time post-stroke, and WAB-R score; χ^2 -test and Fisher's exact test were used to test group difference in race/ethnicity, gender and education)

	Anomic $n_1 = 39$	Broca's $n_2 = 57$	p^*
Age	62.73±11.97	59.82±10.35	0.42
Time post-stroke	2.9±3.42	4.3±4.29	0.13
Race/Ethnicity			0.51
Hispanic	0.00	0.00	
Black	0.13	0.29	
White	0.87	0.68	
Other	0.00	0.03	
Education			0.26
High school	0.07	0.26	
College or associate	0.07	0.09	
Bachelor and above	0.86	0.65	
Gender			0.74
Male	0.60	0.68	
WAB-R	85.74±6.38	46.44±16.93	< 0.01

were then spatially smoothed with a Gaussian kernel with FWHM= 6 mm. To eliminate artifacts driven by lesions, a pipeline proposed by Yourganov et al. (2018) was applied on the rs-fMRI. The FSL MELODIC package was used to decompose the data into independent components (ICs) and to compute the Z-scored spatial maps for the ICs. The spatial maps were thresholded at $p < 0.05$ and compared with the lesion mask for the participant. The Jaccard index, computed as the ratio between the numbers of voxels in the intersection and union, was used to quantify the amount of spatial overlap between the lesion mask and thresholded IC maps, both of which were binary. ICs corresponding to Jaccard index > 5% were deemed significantly overlapping with the lesion mask and then regressed out of the fMRI data using the `fsl_regfilt` script from the FSL package. By applying the atlas of intrinsic connectivity of homotopic areas (AICHA) (Joliot et al. 2015), 384 regions of interest (ROIs) were created.

Lesion-controlled network-based statistic (NBS) analysis

We used the NBS method to identify a subnetwork that differentiates the resting-state connectivity patterns of the anomic and Broca's aphasia groups. It builds on edge-level mass univariate testing with multiple comparison adjustment but refines the approach through breadth-first search.

We first constructed functional connectivity matrices for individual participants using Pearson's correlation between

BOLD signals in the ROIs as edge weight. The Fisher's z -transformation was applied to the coefficients to enforce normality:

$$z = \frac{1}{2} \ln\left(\frac{1+r}{1-r}\right) = \operatorname{arctanh}(r),$$

where r was a correlation coefficient and z was the corresponding normalized correlation coefficient. After normalizing the coefficients, a $p \times p$ connectivity matrix, with $p = 384$ being the number of ROIs in the AICHA atlas, was constructed for each participant in the two aphasia groups. The (i, j) -th entry of such a matrix denotes the weight of an edge or connection between the i th and j th ROIs of the corresponding network. As the connectivity matrices are symmetric, we only included the $p(p-1)/2$ upper or lower triangular entries in the analysis.

We implemented the NBS method through the NBS Connectome toolbox (Reference Manual v1.2, December 2012). It began with mass univariate testing, where we independently tested the hypothesis of group mean indifference at every connection or edge in the network with a two-sample *t*-test. Each connection was then endowed with a single *t*-value quantifying the evidence in favor of the null hypothesis. The second step was thresholding the *t*-values. The connections with a *t*-value exceeding a chosen threshold were admitted to a set of supra-threshold connections. The third step was to identify connected graph components or subnetworks among the set of supra-threshold connections. A connected graph component or subnetwork is a set of supra-threshold connections for which a path can be found between any two nodes in the subnetwork. All connected graph components or subnetworks were identified with the breadth-first search algorithm (Ahuja et al. 1993; Hopcroft and Tarjan 1973). The final step was to compute a familywise error rate (FWER)-corrected p -value for each subnetwork using permutation testing. The basic premise of permutation testing is that the correspondence between data points and their labels can be randomly rearranged under the null hypothesis. An empirical null distribution of the test statistic is then generated through the random label exchanges. Permutation testing is the current 'gold standard' for statistical inference in lesion-symptom mapping investigations, as it relies on minimal statistical assumptions and provides strong protection against false positives (Baldo et al. 2022; Kimberg et al. 2007; Mirman et al. 2018). Similar to cluster-based corrections in voxelwise investigations, the NBS uses permutation control based on the size of the identified subnetwork after setting a preliminary threshold on connection strength. Indeed, prior work using simulated data has demonstrated that the permutation-corrected NBS provides increased true positive detection while maintaining false positive control (Zalesky et al. 2010; Serin et al. 2021).

Our data was permuted at least 5000 times (with a stability check of 1000 permutations in increment). Each permutation involved randomly permuting the data labels according to a permutation vector containing a random permutation of the integers from 1 to the total number of participants in the two groups combined. The same permutation vector was used for every connection to preserve any interdependencies between connections.

Since the brain networks of our aphasic participants are affected by lesions, we included lesion volume as a covariate in the NBS method to control for stroke severity. So the residuals that remained after regressing out lesion volume using a general linear model were permuted instead of the raw data (Freedman and Lane 1983). For each permutation, the first three steps described above were carried out on the permuted data. The size of the largest component was recorded for each permutation, thereby yielding an empirical null distribution for the size of the largest component size. The one-sided FWER-corrected p -value for a component of given size was then estimated as the proportion of permutations for which the largest component was of the same size or greater. The first three steps of the NBS pipeline are illustrated in Figure 3. We also ran a performance evaluation of the general NBS approach, the results of which are summarized in the Appendix.

Properties of subnetwork identified through NBS

We used complex network measures to quantify the topological properties of the subnetwork (Rubinov and Sporns 2010) (Fig. 4). We focused on the functional segregation and centrality measures. Functional segregation is the ability of processing a certain task to occur within densely interconnected ROIs (Rubinov and Sporns 2010). The clustering coefficient is a basic measure of functional segregation based on the number of triangles around a given ROI, where each triangle is formed by the given ROI and two other distinct ROIs, and the three edges connecting them. The clustering coefficient of the ROI quantifies how well connected this ROI's neighbors are, which is equivalent to the number of triangles around the ROI divided by the number of edges that could possibly exist between the ROI and its neighbors. The ROI with a clustering coefficient that is close or equal to 1 implies that the other ROIs in this subnetwork cluster around it. On the other hand, central nodes or hubs are the ROIs with central placement in the overall subnetwork structure. They play an important role in communication and integration in the subnetwork (van den Heuvel and Sporns 2013). Degree, a simple measure of centrality, is defined as the number of edges directly linked to a given ROI. The larger the degree is, the more central the ROI is. Betweenness is another measure of centrality defined at a given ROI as the fraction of all

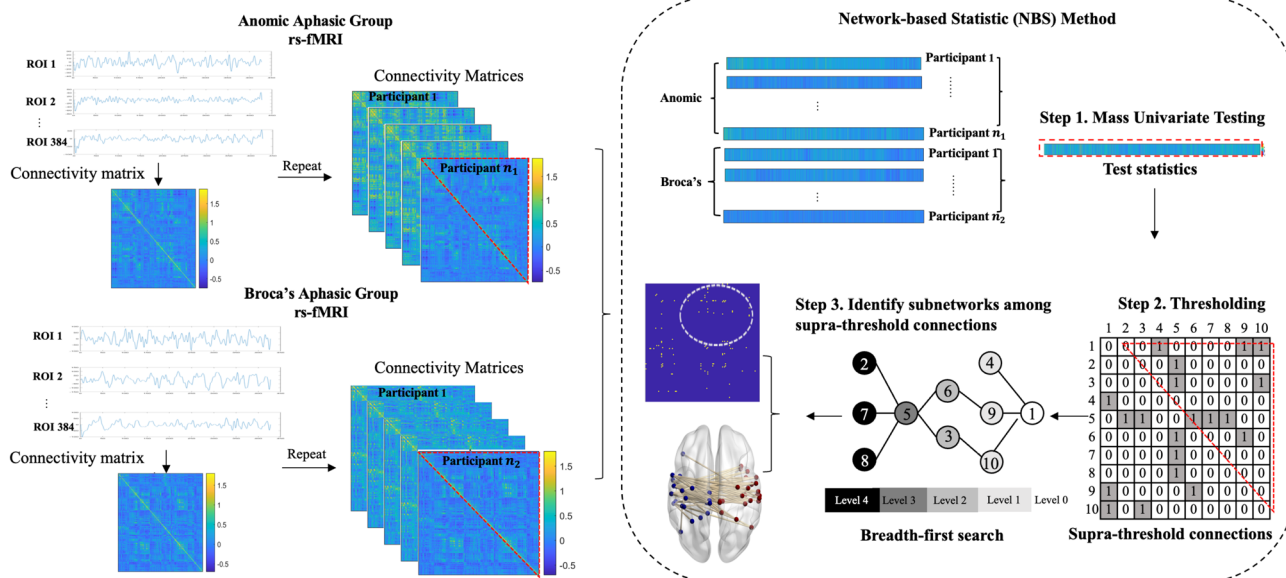
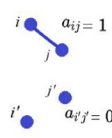


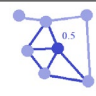

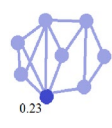


Fig. 3 Left: Resting-state connectivity matrices are constructed from two groups of rs-fMRI data. Right: Illustration of the network-based statistic (NBS) method and how a connected component or subnetwork differentiating the connectivity patterns of the two groups of resting-state functional brain networks is identified through the

breadth-first search algorithm. A permutation test determines the statistical significance of the subnetwork by iterating the three steps at each permutation and compares the permuted statistics with the statistic from the original observed data

Fig. 4 Terminology and examples of basic network measures, clustering coefficient, degree, and betweenness

	Terminology	Example
	<p>D is the set of all ROIs in the subnetwork. p is the number of ROIs. L is the set of suprathreshold edges in the subnetwork.</p> <p>a_{ij} represents the existence of suprathreshold edge between ROI i and j, $i, j \in D$; $a_{ij} = 1$ when a suprathreshold edge exists; $a_{ij} = 0$ otherwise.</p>	
Triangle	<p>Given ROI i, where $i \in D$, the number of triangles around it is calculated by $t_i = \frac{1}{2} \sum_{j,h \in D} a_{ij} a_{ih} a_{jh}$.</p>	
Shortest path length	<p>Shortest path length between ROI i and j, where $i, j \in D$, is calculated by $d_{ij} = \sum_{a_{uv} \in g_{i \leftrightarrow j}} a_{uv}$, where $g_{i \leftrightarrow j}$ is the shortest path between ROI i and j. Note that $d_{ij} = \infty$ when ROI i and j are disconnected.</p>	
Measure of Functional Segregation		
Clustering coefficient	<p>Given ROI i, where $i \in D$, its clustering coefficient is $c_i = \frac{2t_i}{k_i(k_i-1)}$ when $k_i \geq 2$, $c_i = 0$ when $k_i < 2$.</p>	
Measure of Centrality		
Degree	<p>Given ROI i, where $i \in D$, its degree is calculated by $k_i = \sum_{j \in D} a_{ij}$.</p>	
Betweenness	<p>Given ROI i, where $i \in D$, its betweenness is $b_i = \frac{1}{(p-1)(p-2)} \sum_{h,j=N, n \neq j, h \neq j \neq i} \frac{\rho_{hj}(i)}{\rho_{hj}}$, where ρ_{hj} is the number of shortest paths between ROI h and j, $\rho_{hj}(i)$ is the number of shortest paths that pass through ROI i.</p>	

shortest paths in the subnetwork, which are paths with the smallest numbers of edges between two ROIs in the subnetwork, passing through the ROI. An ROI with high betweenness is regarded as a bridge connecting the other ROIs in the subnetwork.

Comparison with standard lesion symptom mapping

For comparison with the NBS results, we used two traditional mass univariate methods: voxel- and connectivity-based lesion symptom mapping (VLSM, CSLM). All analyses included lesion volume as a covariate, and were conducted using NiiStat: <https://www.nitrc.org/projects/niistat/>. For both V- and CSLM, Freedman-Lane regression (Freedman and Lane 1983) was used to contrast the damage or connectivity of the two groups while controlling for lesion volume. Whole brain VLSM was used to identify brain damage associated with aphasia type (anomic or

Broca's). VLSM shows the statistical likelihood that damage to a given voxel is associated with aphasia type group membership, where each voxel in each patient is binarily demarcated as either damaged or undamaged (Bates et al. 2003). We then conducted CLSM (Gleichgerrcht et al. 2017b) using resting-state functional connectivity based on the AICHA atlas, including all left-to-left, left-to-right, and right-to-right connections in the analysis. Only voxels where at least 5 patients had damage were considered, based on the minimum overlap recommendation of 10% of the patient sample (Baldo et al. 2022). All tests were two-tailed, with $\alpha = 0.05$, and significance was determined via permutation testing, where stability of p -value were tested in increments of 1000 permutations, ranging from 1,000 permutation to 10,000 permutations.

For CLSM, we also restricted the analysis to a smaller set of 'dorsal stream' areas, i.e., frontoparietal and superior temporal areas that are involved in form-to-articulation during speech (Fridriksson et al. 2016). These areas would

be hypothesized to be especially disrupted in individuals with Broca's aphasia who struggle with many aspects of speech production compared to the relatively mild anomic cases where the individuals have occasional word-finding difficulties. We included the AICHA ROIs corresponding to supramarginal gyrus, primary sensory and motor cortices, inferior frontal gyrus (Broca's area), insula, superior temporal gyrus, and rolandic operculum. This allowed us to restrict the # of connections while also allowing us to use a one-tailed analysis since we specifically hypothesized these connections would be associated with Broca's aphasia. It is worth noting that we also tried the alternate analysis, using a different set of language regions that might be implicated in anomic aphasia more than Broca's, but this did not reveal any significant results. This is likely because anomic aphasia as a behavioral syndrome may be caused by deficits at various functional levels within the language production system (conceptual, lexical, semantic, phonological, for example), so that similar surface behavior may result from different patterns of neural damage. In addition, in our own sample anomic aphasia was 'less severe' than Broca's aphasia, on average, which would also make the detection of areas specifically related to the anomic group more difficult.

Results

Applying the NBS method to rs-fMRI, we identified a subnetwork distinguishing the anomic and Broca's groups with respect to each of the t-statistic thresholds 3.5, 4, and 4.5. As the threshold increased, the subnetwork size and the number of ROIs contained in the subnetwork decreased (Table 2), until a threshold of 5, at which there was no significant subnetwork. Subsequent results all pertain to the largest subnetwork (threshold 3.5; Fig. 5). All connections in the networks from the group with anomic aphasia were stronger than the networks from the people with Broca's aphasia. The subnetwork was bilateral and involved ROIs in the insula, supramarginal gyrus, and primary motor, sensory, and auditory cortices. In comparison, mass univariate testing with multiple comparisons also identified several connections that were significantly different between the two aphasia groups.

Table 2 The subnetwork identified by the NBS method with t-statistic threshold 3.5, 4, and 4.5, controlling for lesion volume

T-statistic threshold	Number of connections	Number of ROIs	<i>p</i> -value
3.5	74	47	0.03
4.0	22	15	0.01
4.5	5	6	0.01

By comparing the results in the two methods, we found that the majority of significant connections declared by mass univariate testing existed in the subnetwork identified by the NBS with threshold 4 and above. When the threshold in the NBS was less than 4, a large amount of connections in the subnetwork were not detected by mass univariate testing.

For topological properties of the subnetwork identified by NBS with threshold 3.5, the clustering coefficient, degree, and betweenness as described in the previous section were computed. Figures 6, 7 and 8 lists the top 20 nodes with the highest measurement values. The clustering coefficient of the right paracentral lobule and inferior frontal sulcus reached the maximum value of 1, and the bilateral superior temporal gyri, right rolandic operculum, right insula, and left supramarginal gyrus also displayed high clustering coefficients. Regarding the centrality, the left superior temporal gyrus and rolandic operculum had the largest degree. Furthermore, the left superior temporal gyrus, right post-central gyrus, and left rolandic operculum exhibited a high betweenness.

Standard lesion symptom mapping (LSM) results

Whole-brain VLSM, controlling for lesion volume, revealed a cluster of voxels with a peak in the left precentral gyrus and underlying white matter, where damage was significantly associated with Broca's aphasia group membership (peak $z = 7.4$, $p < .001$; Fig. 7). The cluster extended toward the rolandic operculum and inferior frontal sulcus. On the other hand, no connections survived in the whole-brain CLSM analysis. Using a smaller set of AICHA ROIs hypothesized to be more involved in Broca's aphasia than anomic, 10 connections survived that were significantly weaker in the Broca's group (Figure 8). Significant results remained unchanged as we increased the # of permutations from 1,000 up to 10,000. Critical values only changed slightly depending on # of permutations.

Discussion

This study identified functional subnetworks distinguishing anomic and Broca's aphasia. Weaker connectivity of this subnetwork was associated Broca's aphasia when compared to anomic, as classified by the WAB-R. Importantly, connectome-based analyses allowed for the identification of behaviorally relevant nodes in the undamaged right hemisphere, as well as outside of the typical lesion location in the left hemisphere, which cannot be identified when using lesion location alone (VLSM; Fig. 7). Identification of these distributed nodes and links is important for a few reasons. First, it provides information about post-stroke functional organization, which has robust behavioral consequences

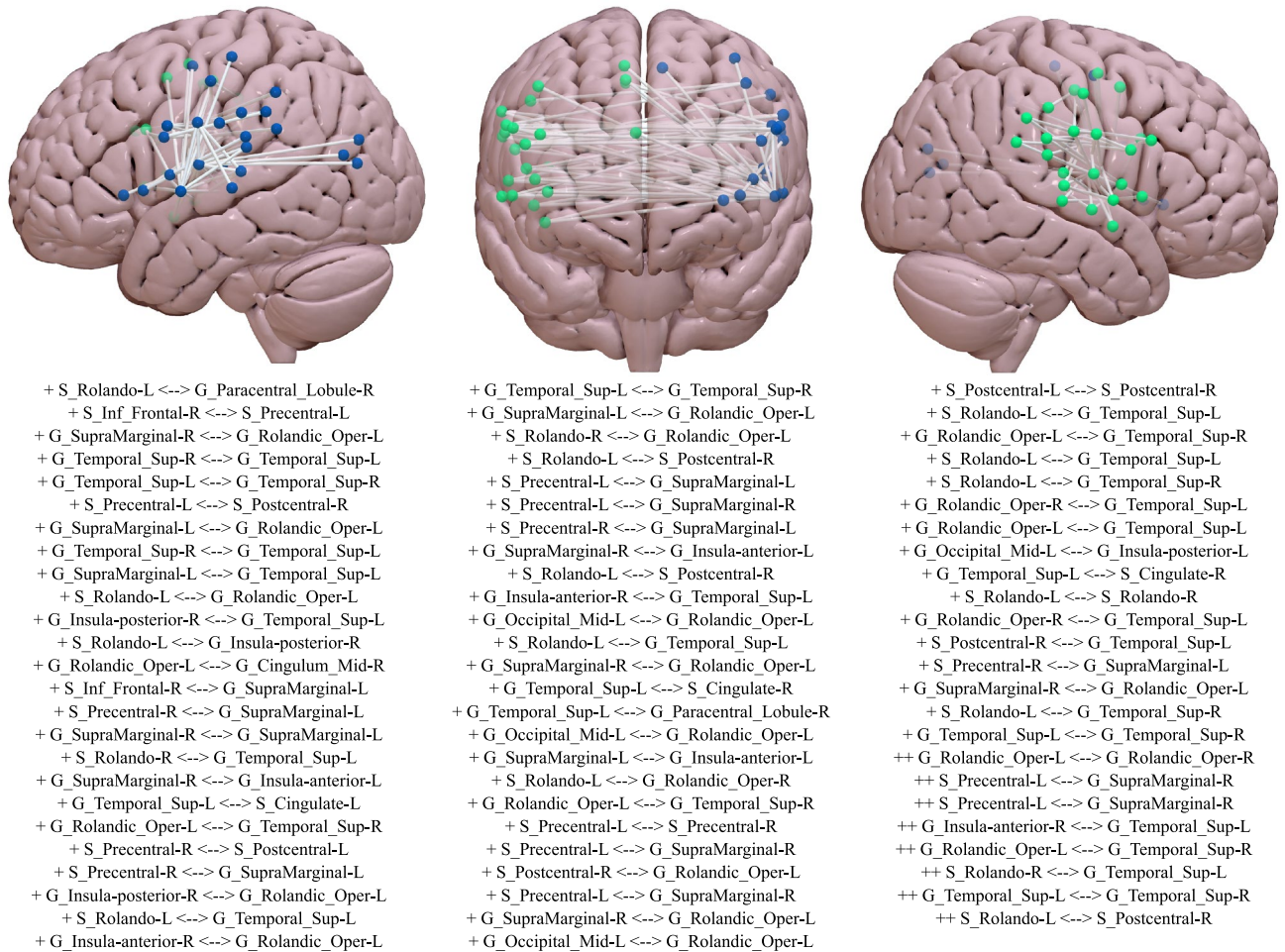


Fig. 5 Connections in the subnetwork identified by the whole-brain NBS method with threshold 3.5, where rs-fMRI connectivity is weaker in the Broca's group. + means the test statistic is in the range

3.5–4.5, ++ means the test statistic > 4.5. Blue nodes indicate left hemisphere, green nodes indicate right

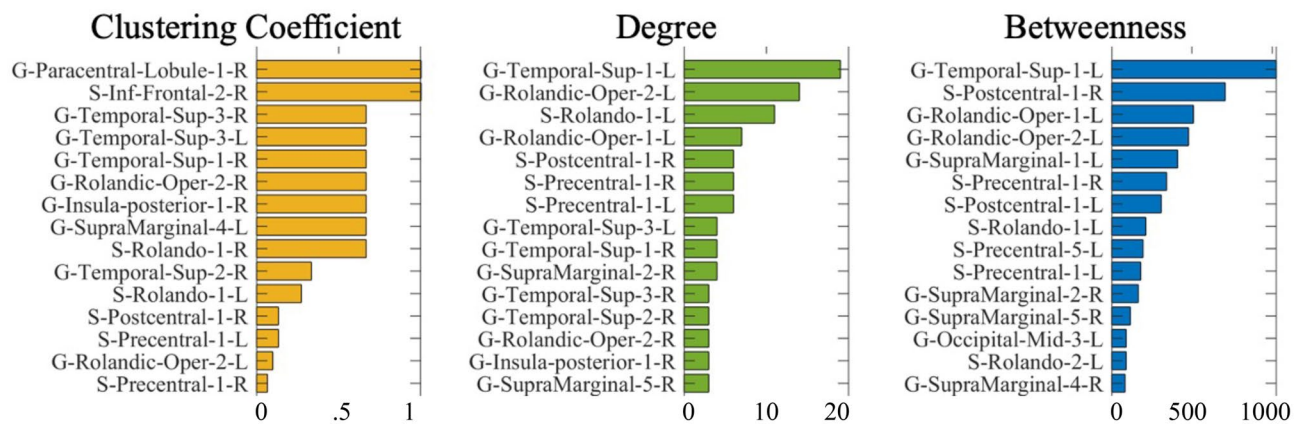


Fig. 6 Top 15 nodes ranked by the complex network measures within the identified subnetwork

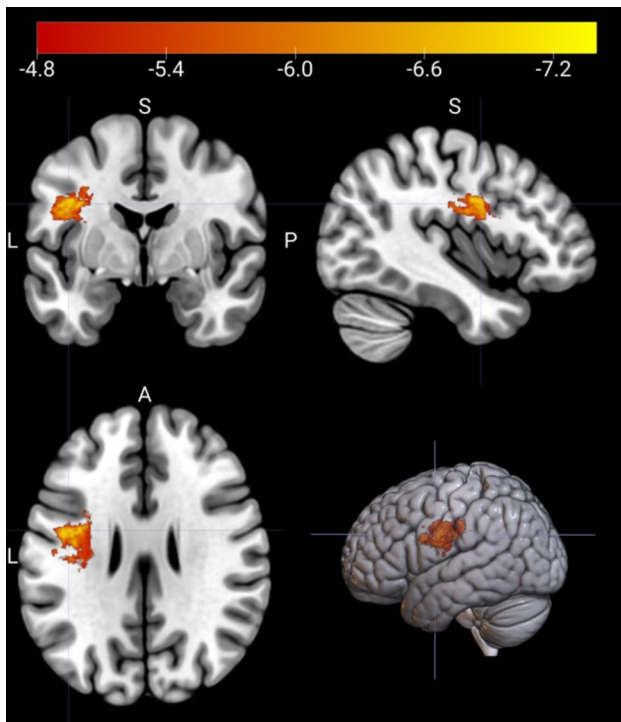


Fig. 7 Whole-brain VLSM cluster where damaged was significantly associated with Broca's aphasia group membership, controlling for lesion volume (peak $z = 7.4$, $p < .001$)

(Siegel et al. 2016; Hartwigsen and Saur 2019; Stockert et al. 2020). Second, it can identify functionally relevant nodes in undamaged tissue that future studies can target with brain stimulation in experimental therapies (Schlaug et al. 2011; Cotelli et al. 2020; Ding et al. 2022). Third, in unilateral stroke, it provides information about contributions related

to the undamaged hemisphere, which has behavioral consequences and cannot be detected using a lesion-only approach (Schneider et al. 2022; Mohr et al. 2014; Heiss 2020)

The subnetwork identified through the NBS method under threshold 4 included bilateral insula, supramarginal gyrus, and primary motor, sensory, and auditory cortices. Studies have shown that precentral gyrus, as well as postcentral, paracentral, and supramarginal gyri, contribute to motor planning and execution (Roux et al. 2020; Schneider 2020; Ma et al. 2011). These regions are involved in encoding complex patterns of motor actions, selecting appropriate motor plans, or controlling a series of movements. In severe Broca's aphasia, damage to this motor planning and execution network can leave the patient with no speech output or only stereotyped output, but relatively intact comprehension (Naeser et al. 1989). However, it should be noted that the WAB-R does not directly measure speech-motor characterizations. NBS and CLSM highlighted the importance of connectivity of bilateral STG, which is vital for auditory processing of speech sounds (Luo and Poeppel 2007; Rolls et al. 2023). A plausible interpretation is that disruption of this motor and auditory network (i.e., the 'dorsal language stream'; (Fridriksson et al. 2018, 2016)) impairs various aspects of sensory-motor integration and motor planning/execution that are vital for speech production (Hickok 2012), resulting in the disfluency that is characteristic of Broca's aphasia.

Another finding is that the identified connections are largely bilateral instead of left hemisphere dominant. ROIs located in the right paracentral lobule and inferior frontal sulcus, as well as bilateral STG, were identified using network measures of functional segregation. While this reflects the intrinsic bilaterality of resting state networks (Lee et al. 2013; Smitha et al. 2017), it also suggests that connectivity

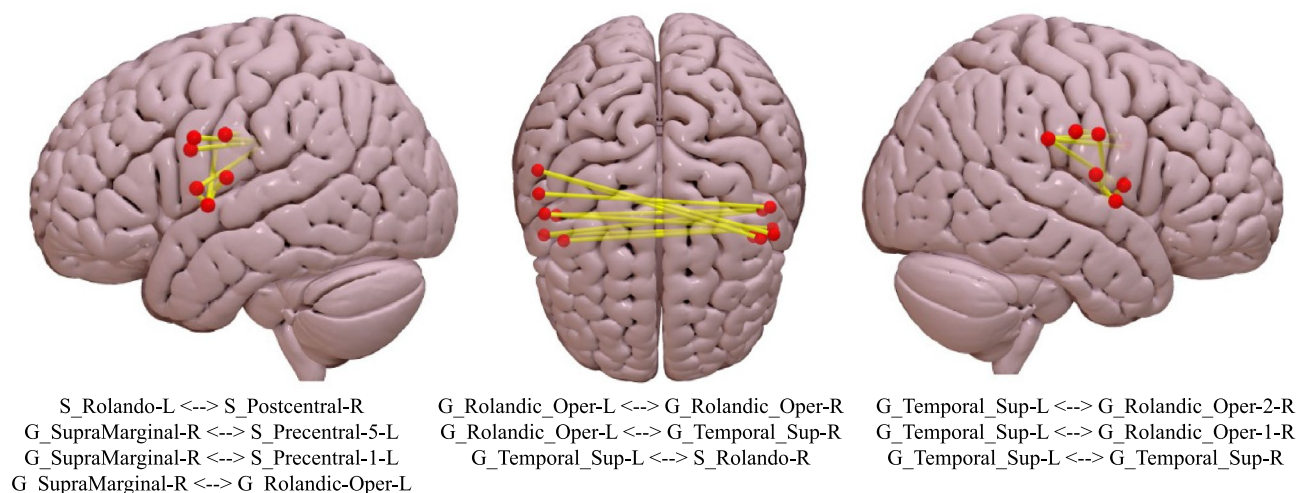


Fig. 8 No rs-FMRI connections survived whole-brain CLSM. These 10 connections survived when restricting CLSM to 80 (out of 384) regions of interest, indicating where rs-FMRI is weaker in the Broca's group after controlling for lesion volume

and clustering around right hemisphere dorsal stream areas have behavioral consequences post-stroke. Using measures of centrality, the degree of the ROIs in the left STG and rolandic operculum shows more connections linking to them than to other ROIs in the subnetwork. Additionally, the results of betweenness suggest that the left STG and rolandic operculum, as well as right postcentral gyrus, play a crucial role in information flow and overall communication efficiency in the subnetwork and comprise the bridge connecting to other ROIs.

Taken together, these results revealed a surprising role of right hemisphere nodes when distinguishing Broca's from anomic aphasia. Preserved connectivity of a tightly connected, bilateral subnetwork with central nodes in the right primary sensory and motor cortices was associated with membership in the comparatively milder anomic group. While disruption of this network is ultimately caused by left hemisphere damage in this group of participants, it nonetheless suggests that the quality of right hemisphere connectivity is an important feature of post-stroke language outcomes. These results are consistent with the view that the right hemisphere provides some degree of redundancy to left hemisphere language functions. When left hemisphere areas and left-to-left connections are damaged, some degree of compensation may be provided by right hemisphere inputs when left-to-right connections are intact. When left-to-right connections are also damaged, more severe impairments are observed. This aligns well with other recent studies demonstrating the importance of connectivity to the right hemisphere following left hemisphere damage (Riccardi et al. 2020, 2019; Yourganov et al. 2021), and suggests that facilitation of right hemisphere connectivity could be a goal for future studies seeking to improve cognitive or behavioral outcomes in survivors of stroke (Desowska and Turner 2019; Watson et al. 2019).

Finally, complex network measures also revealed the importance of the left supramarginal gyrus (SMG) in this subnetwork, with the SMG having the fifth highest betweenness. The left SMG is important for auditory-verbal short-term memory (Deschamps et al. 2014), phonological processing (Oberhuber et al. 2016), and has been proposed as an auditory-motor interface that is vital for speech and articulation (Hickok et al. 2009). Our findings support the idea that the left SMG is a central node in speech production, and suggest that disruption of this node contributes to the symptoms of Broca's aphasia.

An interesting negative result is the absence of significant connections (or voxels in VLSM) from what is traditionally referred to as "Broca's area" (e.g., left inferior frontal cortex (IFC); (Keller et al. 2009)). Although caution is warranted when interpreting negative results, one possibility is that disruption of IFC contributes to the symptoms of both anomic and Broca's aphasia and does not statistically

distinguishing the two groups of people. Indeed, the IFC and its subregions have a wide range of proposed language-specific and domain-general functions (Rogalsky and Hickok 2011; Fadiga et al. 2009; Grodzinsky and Santi 2008), and functional organization of IFC has high variability between individuals (Fedorenko and Blank 2020). Disruption could therefore give rise to a range of symptoms, not just those specifically associated with Broca's aphasia. Another possibility is that disruption of "Broca's area" is not necessary to display the symptoms of Broca's aphasia. This aligns with research suggesting that disruption of other areas, such as posterior STG and insula, are powerful predictors of Broca's aphasia symptoms (Fridriksson et al. 2015; Dronkers et al. 2007), and that Broca's aphasia can present without damage to Broca's area proper (Fridriksson et al. 2007; Ardila et al. 2016).

For qualitative comparison to NBS, we also ran standard permutation-corrected VLSM and CLSM, where CLSM is most closely related to NBS in its connection-based inference approach. No connection survived the whole-brain CLSM, whereas whole-brain NBS revealed significant subnetworks at a range of thresholds. We then restricted CLSM to a smaller set of regions hypothesized to be more involved in Broca's aphasia than anomic. Ten bilateral connections, which resembled a subset of the NBS subnetwork, survived this restricted CLSM analysis. These results suggest that, when conducting a whole-brain analysis with thousands of connections, NBS may provide greater sensitivity, while maintaining robust control of false positives (Zalesky et al. 2010), and allow exploration of large networks and their features. However, CLSM is likely more appropriate for use within a restricted, hypothesis-driven network of interest for two reasons. First, as demonstrated by (Zalesky et al. 2010), NBS's power advantage over CLSM scales as potential network size increases, but NBS is powerless to detect effects related to single, isolated links as opposed to connected subnetworks. Second, due to differences in the permutation control procedure between NBS and CLSM (i.e., controlling based on subnetwork size or each individual link, respectively), CLSM allows for strong claims about the significance of individual links. This is advantageous when the analysis is restricted to a subset of a priori links that are hypothesized to be related to the behavior of interest.

Limitations and future directions

The present study focused on Broca's and anomic aphasia. One reason for this was sample size, with other types of aphasia being comparatively underrepresented at our center. As such, we cannot strongly claim that the results presented here are specific to Broca's aphasia, as comparing other aphasia types to anomic aphasia may reveal similar

subnetworks. Future studies could seek to use NBS to compare the neural correlates of other types of aphasia. Also due to sample size, we did not leverage multivariate LSM, as recent work recommends that reliable multivariate LSM models require data from hundreds or even thousands of participants (Sperber et al. 2019; Ivanova et al. 2021; Karnath et al. 2018; Mah et al. 2014). Future work with larger samples could apply multivariate techniques when comparing the anatomical correlates of aphasia subtypes.

While we controlled for total lesion volume in all analyses, the resting-state connectomes used in the current study are informed by a complex set of interacting features such as location of necrotic tissue (Manan et al. 2020), hypoperfusion (Zhang et al. 2019), white matter hyperintensities (Vettore et al. 2021), brain health in surviving tissue (Wilmskoetter et al. 2023; Stumme et al. 2022), etc. Future work could seek to investigate how these features relate to functional connectivity in post-stroke aphasia or, alternatively, to statistically orthogonalize behavioral contributions of brain structure vs. function. As such, we do not seek to make claims about the etiology of the functional connectomes observed here.

We did not find any evidence of connections that were weaker in the anomic group. The reason for this is likely that: (1) word-finding difficulties can be observed after damage to a wide range of regions (Dronkers and Baldo 2009), reducing the likelihood of finding a common neural substrate at the group level, and (2) our anomic participants were less impaired and had more subtle language deficits than the group with Broca's aphasia. Although differences in severity can be partially accounted for by including lesion size as a covariate, as was done here, it is simply more difficult to identify the neural correlates of relatively mild symptoms. Relatedly, as mentioned in the Introduction, grouping participants based on WAB-R aphasia classification may not be ideal, as there can be significant behavioral variability between participants within the same classification. An alternative is to use a data-driven dimension reduction approach such as principal component analysis to group participants or correlated symptoms together (Stefaniak et al. 2022), although this method also has its own drawbacks (Walker and Hickok 2023).

One of the advantages of the NBS method is controlling the FWER at a subnetwork level; while the standard mass univariate testing approach is controlling at individual connection independently, which ignores the interactions among ROIs. If suprathreshold edges form a subnetwork, the NBS method provides substantially greater power (Zalesky et al. 2010). Nevertheless, if ROIs are not connected by suprathreshold edges and thus cannot form a subnetwork, the NBS method will fail to make any decision. Under a

network framework, once the NBS identifies any subnetwork, it would allow us to study their network topology and make straightforward interpretations. These findings may be somewhat limited by not taking into account the effect sizes and significance of the differences. For instance, after a threshold is applied, the weight for suprathreshold edges would all set to 1. In future investigations, it may be possible to use weighted edges for a continuous analysis. On the other hand, the critical factor affecting the subnetwork size and determining whether suprathreshold edges would form a subnetwork is the threshold in the NBS method.

Under different thresholds, new subnetwork(s) with fewer or more functional connections may be identified, and the *p*-value of the subnetwork(s) may change and result in a loss of significance. To address the concern of threshold, we examined a range of thresholds in the NBS method and incorporated the baseline approach in our analysis. The functional connections are significant across both the NBS method with a range of thresholds and the baseline approach, which implies notable differences in functional connectivity between anomic and Broca's aphasia. For future studies, the NBS method can be combined with a data-driven threshold selection. We can also explore multiscale topological network models to overcome the arbitrary thresholding issue (Wang et al. 2022).

Conclusion

Here, we used VLSM, CLSM, and the NBS to examine neural correlates that distinguish anomic and Broca's aphasia. Whole-brain NBS identified a subnetwork located in the dorsal language stream bilaterally, including supramarginal gyrus, primary sensory, motor, and auditory cortices, and insula. The connections among these areas are weaker in Broca's aphasia than anomic aphasia. By examining network properties, we found that (1) the right paracentral gyrus, right inferior frontal sulcus, and bilateral STG display high clustering coefficients, and (2) the left auditory cortex, left SMG, and right primary sensory cortex exhibit high centrality, serving as connection hubs within the subnetwork. These findings suggest that the disruptions of these nodes and their connections are associated with Broca's aphasia symptoms. CLSM corroborated these results, but only when restricting the analysis to a smaller a priori network of interest. This suggests that NBS is more sensitive than traditional CLSM when conducting a connectome-based analysis with thousands of edges, and that NBS allows for the identification of larger networks and additional features than CLSM.

Appendix. Performance evaluation of NBS

For baseline comparison with the NBS method, mass univariate permutation testing with multiple comparison was performed. The p -value for comparing the j th edge weight was calculated by $Pr(|t_j^*| \geq |t_j|)$, where t_j^* and t_j were the test statistics computed from permuted data and original data respectively. This p -value describes how likely the absolute value of test statistic from permuted data exceeds the absolute value of test statistic from original data. Then, the following multiple comparison procedures were applied to correct multiple p -values and control the FWER: Bonferroni correction (Bonferroni 1936), Holm's Bonferroni correction (Holm 1979), and false discovery rate (FDR) control (Benjamini and Hochberg 1995).

We used three simulation studies to evaluate the empirical performance of the NBS method against mass univariate testing with multiple comparison. We assessed two aspects of the performance: (1) sensitivity or true positive rate (TPR): the proportion of connections or edges containing group differences that are correctly identified; (2) 1-specificity or false positive rate (FPR): the proportion of edges without differences that are misclassified. Ideally, $TPR = 1$ (all edges that differ between the two groups are identified), and $FPR = 0$ (all edges that do not differ between the two groups are not identified). Suppose H is the set of edges that differ between the groups, R is the set of edges that do not differ between the groups, and \hat{h} is the set of edges

comprising the subnetwork identified by a specific method (NBS, baseline mass univariate testing with multiple comparison). The TPR was then calculated by $|H \cap \hat{h}|/|\hat{h}|$ and the FPR by $|R \cap \hat{h}|/|\hat{h}|$.

In each of the three studies, we generated two groups of p -node networks. The group sizes are $n_1 = n_2 = 10$ for all three studies. In each network, the weight of the edge between node i and j was generated by $w_{ij} \sim N(\text{arctanh}(r_{ij}), \sigma_w^2)$ with $r_{ij} \sim U(-1, 1)$ and $\sigma_w = 1/\sqrt{p(p-1)/2-3}$. We randomly chose $C_r\%$ of $p(p-1)/2$ edges to differ in weights between Group 1 and 2, and refer to these edges as *contrast edges*. The weights of contrast edges were generated independently with

$$w_{ij}^* = \begin{cases} w_{ij} + w^*, & \text{for } w_{ij} \geq 0 \\ w_{ij} - w^*, & \text{for } w_{ij} < 0, \end{cases}$$

where $w^* \sim N(0.03, 0.01)$. We compared the performance of the methods via different p and C_r values in the three studies.

Study 1. $p = 20$ and $C_r\% = 10\%$.

Study 2. $p = 40$ and $C_r\% = 10\%$.

Study 3. $p = 40$ and $C_r\% = 5\%$.

After the networks were generated, NBS with threshold 2.5 and mass univariate testing with multiple comparison were performed (Fig. 9). We repeated the simulation process

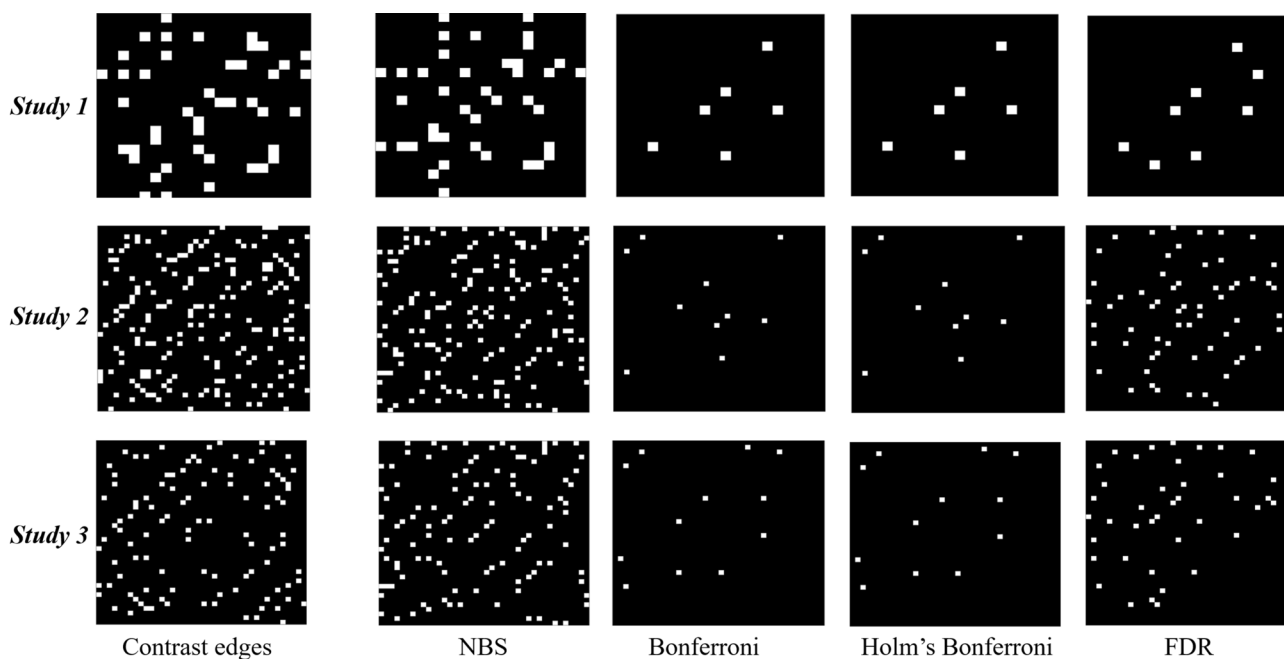


Fig. 9 Simulation setup: The white blocks in the left side's matrices represent contrast edges, whose weights differ between the two groups. The white blocks in the right side's matrices are the subnet-

work or connected component identified by the NBS method or the edges declared significant by multiple comparison

Table 3 The average TPR and FPR of the NBS with threshold 2.5 and mass univariate testing with multiple comparison, in 5,000 simulations

(p, C_r)		NBS	Mass Univariate Testing		
			Bonf.	Holm's	FDR
Study 1 (20, 10)	TPR	0.7278	0.2538	0.2538	0.5896
	FPR	0.0089	0.0002	0.0002	0.0016
Study 2 (40, 10)	TPR	0.9557	0.5670	0.5670	0.9431
	FPR	0.0103	0.0001	0.0001	0.0024
Study 3 (40, 5)	TPR	0.9317	0.5687	0.5687	0.9270
	FPR	0.0104	0.0001	0.0001	0.0012

5,000 times for each study. Average TPR and FPP were computed respectively.

Simulation results

Table 3 summarizes results of the three simulation studies. In Study 1, the NBS method has the largest TPR and FPR, while the mass univariate testing with FDR detects a desirable proportion of contrast edges and contains a small number of false discoveries. In Study 2, as the network size expands, the TPRs by the NBS and mass univariate testing methods increase, whereas the FPRs increase by the NBS and FDR methods and decrease by the Bonferroni and Holm's Bonferroni methods. In Study 3, when fewer contrast edges are placed in either of the two groups, the TPRs by the NBS and FDR methods decrease and the FPRs by the NBS and the two Bonferroni corrections stay similar to Study 2.

In summary, compared with mass univariate testing, the NBS method detects small group differences well under various network sizes and proportions of contrast edges. For the mass univariate testing, the FDR has the highest power and a favorable FPR; Bonferroni and Holm's Bonferroni corrections are highly conservative in detecting contrast edges. Additionally, we find that the computation speed is mainly affected by network size.

Acknowledgements The authors would like to thank Makayla Gibson at the University of South Carolina for facilitating access to the dataset used in this study.

Author Contributions Conceptualization (XZ, YW, JF). Study design and data acquisition (JF). Statistical analysis (XZ, NR). Interpretation of results (XZ, YW, NR, DdO, RHD). Writing and editing (All).

Funding RHD: NIH R01DC017162 and R01DC01716202S1. JF: NIH R21-DC014170 and P50-DC014664.

Data availability The datasets generated during and analyzed during the current study are available from the corresponding author on reasonable request.

Declarations

Conflict of interest None.

Ethical approval The research was approved by the Institutional Review Board (IRB) at the University of South Carolina.

References

- Ahuja RK, Magnanti TL, Orlin JB (1993) Network flows: theory, algorithms, and applications. Prentice Hall, New Jersey
- Ardila A, Bernal B, Rosselli M (2016) Why broca's area damage does not result in classical broca's aphasia. *Front Human Neurosci* 10:249
- Baldo J, Ivanova M, Herron T, Wilson S, Dronkers N (2022) Voxel-based lesion symptom mapping. In: *Lesion-to-symptom mapping* (pp. 95 - 118)
- Bates E, Wilson S, Saygin A, Dick F, Sereno M, Knight R, Dronkers N (2003) Voxel-based lesion-symptom mapping. *Nat Neurosci* 6:448–450
- Benjamini Y, Hochberg Y (1995) Controlling the false discovery rate: A practical and powerful approach to multiple testing. *J R Stat Soc Ser* 57(1):289–300
- Blackett DS, Varkey J, Wilmskoetter J, Roth R, Andrews K, Busby N et al (2022) Neural network bases of thematic semantic processing in language production. *Cortex* 156:126–143
- Bonferroni CE (1936) Teoria statistica delle classi e calcolo delle probabilità. Libreria Internazionale Seeber
- Broca P (1861) Remarques sur le siège de la faculté du langage articulé, suivies d'une observation d'aphémie (perte de la parole). *Bulletin et Memoires de la Societe anatomique de Paris* 6:330–357
- Caplan D, Alpert N, Waters G, Olivieri A (2000) Activation of broca's area by syntactic processing under conditions of concurrent articulation. *Human Brain Mapping* 9(2):65–71
- Caramazza A, Berndt RS (1978) Semantic and syntactic processes in aphasia: A review of the literature. *Psychol Bull* 85(4):898–918
- Carrera E, Tononi G (2014) Diaschisis: past, present, future. *Brain* 137(9):2408–2422
- Casilio M, Rising K, Beeson PM, Bunton K, Wilson SM (2019) Auditory-perceptual rating of connected speech in aphasia. *Am J Speech Lang Pathol* 28(2):550–568
- Cotelli M, Manenti R, Ferrari C, Gobbi E, Macis A, Cappa SF (2020) Effectiveness of language training and non-invasive brain stimulation on oral and written naming performance in primary progressive aphasia: A meta-analysis and systematic review. *Neurosci Biobehav Rev* 108:498–525
- Den Ouden DB, Malyutina S, Basilakos A, Bonilha L, Gleichgerricht E, Yourganov G, Fridriksson J (2019) Cortical and structural-connectivity damage correlated with impaired syntactic processing in aphasia. *Human Brain Mapping* 40(7):2153–2173
- Desai, R. H. , Riccardi, N. (2021). Cognitive neuroscience of language. *The Routledge handbook of cognitive linguistics* 615–642
- Deschamps I, Baum SR, Gracco VL (2014) On the role of the supra-marginal gyrus in phonological processing and verbal working memory: evidence from rtms studies. *Neuropsychologia* 53:39–46
- Desowska A, Turner DL (2019) Dynamics of brain connectivity after stroke. *Rev Neurosci* 30(6):605–623
- Ding, X. , Zhang, S. , Huang, W. , Zhang, S. , Zhang, L. , Hu, J. et al. (2022). Comparative efficacy of non-invasive brain stimulation for post-stroke aphasia: a network meta-analysis and

- meta-regression of moderators. *Neuroscience & Biobehavioral Reviews* 104804
- Dronkers NF, Baldo JV (2009) Language: Aphasia. In: Squire LR (ed) *Encyclopedia of neuroscience*. Academic Press, Oxford, pp 343–348
- Dronkers NF, Plaisant O, Iba-Zizen MT, Cabanis EA (2007) Paul broca's historic cases: high resolution mr imaging of the brains of leborgne and lelong. *Brain* 130(5):1432–1441
- Dronkers NF, Wilkins DP, Valin RV, Redfern BB, Jaeger J (2004) Lesion analysis of the brain areas involved in language comprehension. *Cognition* 92:145–177
- Fadiga L, Craighero L, D'Ausilio A (2009) Broca's area in language, action, and music. *Ann N Y Acad Sci* 1169(1):448–458
- Fedorenko E, Blank IA (2020) Broca's area is not a natural kind. *Trends Cognitiv Sci* 24(4):270–284
- Fiebach CJ, Schubotz RI (2006) Dynamic anticipatory processing of hierarchical sequential events: a common role for broca's area and ventral premotor cortex across domains? *Cortex* 42(4):499–502
- Fox MD, Raichle ME (2007) Spontaneous fluctuations in brain activity observed with functional magnetic resonance imaging. *Nat Rev Neurosci* 8:700–711
- Freedman D, Lane D (1983) A nonstochastic interpretation of reported significance levels. *J Bus Econ Stat* 1(4):292–298
- Fridriksson J, Bonilha L, Rorden C (2007) Severe broca's aphasia without broca's area damage. *Behavioural neurology* 18(4):237–238
- Fridriksson J, den Ouden DB, Hillis AE, Hickok G, Rorden C, Basilakos A, Bonilha L (2018) Anatomy of aphasia revisited. *Brain* 141(3):848–862
- Fridriksson J, Den Ouden DB, Hillis AE, Hickok G, Rorden C, Basilakos A, Bonilha L (2018) Anatomy of aphasia revisited. *Brain* 141(3):848–862
- Fridriksson J, Fillmore P, Guo D, Rorden C (2015) Chronic broca's aphasia is caused by damage to broca's and wernicke's areas. *Cerebral Cortex* 25(12):4689–4696
- Fridriksson J, Yourganov G, Bonilha L, Basilakos A, den Ouden DB, Rorden C (2016) Revealing the dual streams of speech processing. *Proceedings of the National Academy of Sciences* 113:15108–15113
- Friedmann N (2009) Speech production in broca's agrammatic: aphasia Syntactic tree pruning. In: Grodzinsky Y, Amunts K (eds) *Broca's region*, 3rd edn. Oxford University Press, United Kingdom, pp 63–82
- Gleichgerrcht E, Fridriksson J, Rorden C, Bonilha L (2017) Connectome-based lesion-symptom mapping (clsm): A novel approach to map neurological function. *NeuroImage: Clinical* 16:461–467
- Gleichgerrcht E, Fridriksson J, Rorden C, Bonilha L (2017) Connectome-based lesion-symptom mapping (clsm): A novel approach to map neurological function. *NeuroImage: Clinical* 16:461–467
- Goodglass H, Barresi B, Kaplan E (2001) The assessment of aphasia and related disorders. In, 3rd edn. Lippincott Williams & Wilkins, Philadelphia
- Grodzinsky Y, Santi A (2008) The battle for broca's region. *Trends in cognitive sciences* 12(12):474–480
- Guo J, Yang M, Biswal BB, Yang P, Liao W, Chen H (2019) Abnormal functional connectivity density in post-stroke aphasia. *Brain Topography* 32(2):271–282
- Hartwigsen G, Saur D (2019) Neuroimaging of stroke recovery from aphasia-insights into plasticity of the human language network. *Neuroimage* 190:14–31
- Heiss, W. D. (2020). Mapping of recovery from poststroke aphasia: comparison of pet and fmri. *fMRI: Basics and Clinical Applications* 225–239
- Hickok G (2009) The functional neuroanatomy of language. *Physics of life reviews* 6(3):121–143
- Hickok G (2012) Computational neuroanatomy of speech production. *Nature reviews neuroscience* 13(2):135–145
- Hickok G, Okada K, Serences JT (2009) Area spt in the human planum temporale supports sensory-motor integration for speech processing. *Journal of neurophysiology* 101(5):2725–2732
- Hillis AE (2007) Aphasia: progress in the last quarter of a century. *Neurology* 69(2):200–213
- Hjelmervik H, Hausmann M, Osnes B, Westerhausen R, Specht K (2014) Resting states are resting traits - an fmri study of sex differences and menstrual cycle effects in resting state cognitive control networks. *PLOS ONE* 9(7):1–10
- Holm S (1979) A simple sequentially rejective multiple test procedure. *Scandinavian Journal of Statistics* 6(2):65–70 (<http://www.jstor.org/stable/4615733>)
- Hopcroft J, Tarjan R (1973) Algorithm 447: Efficient algorithms for graph manipulation. *Commun. ACM* 16(6):372–378
- Ivanova MV, Herron TJ, Dronkers NF, Baldo JV (2021) An empirical comparison of univariate versus multivariate methods for the analysis of brain-behavior mapping. *Human Brain Mapping* 42(4):1070–1101
- Joliot, M., Jobard, G., Naveau, M., Delcroix, N., Petit, L., Zago, L., Tzourio-Mazoyer, N. (2015). Aicha: An atlas of intrinsic connectivity of homotopic areas. *Journal of neuroscience methods* 254
- Karnath HO, Sperber C, Rorden C (2018) Mapping human brain lesions and their functional consequences. *Neuroimage* 165:180–189
- Keller SS, Crow T, Foundas A, Amunts K, Roberts N (2009) Broca's area: nomenclature, anatomy, typology and asymmetry. *Brain and language* 109(1):29–48
- Kertesz A (2007) *Wab-r: Western aphasia battery-revised*. PsychCorp, San Antonio, TX
- Kimberg DY, Coslett HB, Schwartz MF (2007) Power in voxel-based lesion-symptom mapping. *Journal of cognitive neuroscience* 19(7):1067–1080
- Lee MH, Smyser CD, Shimony JS (2013) Resting-state fmri: a review of methods and clinical applications. *American Journal of neuroradiology* 34(10):1866–1872
- Luo H, Poeppel D (2007) Phase patterns of neuronal responses reliably discriminate speech in human auditory cortex. *Neuron* 54(6):1001–1010
- Ma L, Narayana S, Robin DA, Fox PT, Xiong J (2011) Changes occur in resting state network of motor system during 4 weeks of motor skill learning. *Neuroimage* 58(1):226–233
- Maas MB, Lev MH, Ay H, Singhal AB, Greer DM, Smith WS, Furie KL (2012) The prognosis for aphasia in stroke. *Journal of Stroke and Cerebrovascular Diseases* 21(5):350–357
- Mah YH, Husain M, Rees G, Nachev P (2014) Human brain lesion-deficit inference remapped. *Brain* 137(9):2522–2531
- Manan HA, Franz EA, Yahya N (2020) Functional connectivity changes in patients with brain tumours-a systematic review on resting state-fmri. *Neurology, Psychiatry and Brain Research* 36:73–82
- Matchin W, Hickok G (2020) The Cortical Organization of Syntax. *Cerebral Cortex* 30(3):1481–1498
- Miceli G, Silveri M, Nocetini U, Caramazza A (1988) Patterns of dissociation in comprehension and production of nouns and verbs. *Aphasiology* 2:351–358
- Mirman D, Landrigan JF, Kokolis S, Verillo S, Ferrara C, Pustina D (2018) Corrections for multiple comparisons in voxel-based lesion-symptom mapping. *Neuropsychologia* 115:112–123
- Mohr B, Difrancesco S, Harrington K, Evans S, Pulvermüller F (2014) Changes of right-hemispheric activation after constraint-induced, intensive language action therapy in chronic aphasia: fmri evidence from auditory semantic processing. *Frontiers in Human Neuroscience* 8:919
- Mohr JP, Pessin MS, Finkelstein S, Funkenstein HH, Duncan GW, Davis KR (1978) Broca aphasia. *Neurology* 28(4):311–311

- Naeser MA, Palumbo CL, Helm-Estabrooks N, Stiassny-Eder D, Albert ML (1989) Severe nonfluency in aphasia: Role of the medial subcallosal fasciculus and other white matter pathways in recovery of spontaneous speech. *Brain* 112(1):1–38
- Oberhuber M, Hope T, Seghier ML, Parker Jones O, Prejawa S, Green DW, Price CJ (2016) Four functionally distinct regions in the left supramarginal gyrus support word processing. *Cerebral Cortex* 26(11):4212–4226
- Ogawa S, Tank DW, Menon R, Ellermann JM, Kim SG, Merkle H, Ugurbil K (1992) Intrinsic signal changes accompanying sensory stimulation: Functional brain mapping with magnetic resonance imaging. *Proceedings of the National Academy of Sciences of the United States of America* 89(13):5951–5955
- Riccardi N, Rorden C, Fridriksson J, Desai RH (2022) Canonical sentence processing and the inferior frontal cortex: Is there a connection? *Neurobiology of Language* 3(2):318–344
- Riccardi N, Yourganov G, Rorden C, Fridriksson J, Desai R (2020) Degradation of praxis brain networks and impaired comprehension of manipulable nouns in stroke. *Journal of Cognitive Neuroscience* 32(3):467–483
- Riccardi N, Yourganov G, Rorden C, Fridriksson J, Desai RH (2019) Dissociating action and abstract verb comprehension post-stroke. *Cortex* 120:131–146
- Robson H, Zahn R, Keidel JL, Binney RJ, Sage K, Lambon Ralph MA (2014) The anterior temporal lobes support residual comprehension in wernicke's aphasia. *Brain* 137(3):931–943
- Rogalsky C, Hickok G (2011) The role of broca's area in sentence comprehension. *Journal of Cognitive Neuroscience* 23(7):1664–1680
- Rogers BP, Morgan VL, Newton AT, Gore JC (2001) Assessing functional connectivity in the human brain by fmri. *Magnetic resonance imaging* 25(10):1347–1357
- Rolls ET, Rauschecker JP, Deco G, Huang CC, Feng J (2023) Auditory cortical connectivity in humans. *Cerebral Cortex* 33(10):6207–6227
- Roux FE, Niare M, Charni S, Giussani C, Durand JB (2020) Functional architecture of the motor homunculus detected by electrostimulation. *The Journal of physiology* 598(23):5487–5504
- Rubinov M, Sporns O (2010) Complex network measures of brain connectivity: Uses and interpretations. *NeuroImage* 52(3):1059–1069
- Schlaug G, Marchina S, Wan CY (2011) The use of non-invasive brain stimulation techniques to facilitate recovery from post-stroke aphasia. *Neuropsychology review* 21:288–301
- Schneider DM (2020) Reflections of action in sensory cortex. *Current opinion in neurobiology* 64:53–59
- Schneider HR, Wawrzyniak M, Stockert A, Klingbeil J, Saur D (2022) fmri informed voxel-based lesion analysis to identify lesions associated with right-hemispheric activation in aphasia recovery. *NeuroImage: Clinical* 36:103169
- Serin E, Zalesky A, Matory A, Walter H, Kruschwitz JD (2021) Nbs-predict: A prediction-based extension of the network-based statistic. *NeuroImage* 244:118625
- Siegel JS, Ramsey LE, Snyder AZ, Metcalf NV, Chacko RV, Weinberger K, Corbetta M (2016) Disruptions of network connectivity predict impairment in multiple behavioral domains after stroke. *Proceedings of the National Academy of Sciences of the United States of America* 113:E4367–E4376
- Smitha K, Akhil Raja K, Arun K, Rajesh P, Thomas B, Kapilamoorthy T, Kesavadas C (2017) Resting state fmri: A review on methods in resting state connectivity analysis and resting state networks. *The neuroradiology journal* 30(4):305–317
- Spell LA, Richardson JD, Basilakos A, Stark BC, Teklehaimanot A, Hillis AE, Fridriksson J (2020) Developing, implementing, and improving assessment and treatment fidelity in clinical aphasia research. *American Journal of Speech-Language Pathology* 29(1):286–298
- Sperber, C., Wiesen, D., Karnath, H. O. (2019). An empirical evaluation of multivariate lesion behaviour mapping using support vector regression (Tech. Rep.). Wiley Online Library
- Stefaniak JD, Geranmayeh F, Lambon Ralph MA (2022) The multidimensional nature of aphasia recovery post-stroke. *Brain* 145(4):1354–1367
- Stockert A, Wawrzyniak M, Klingbeil J, Wrede K, Kümmerer D, Hartwigsen G, Saur D (2020) Dynamics of language reorganization after left temporo-parietal and frontal stroke. *Brain* 143(3):844–861
- Stumme J, Krämer C, Miller T, Schreiber J, Caspers S, Jockwitz C (2022) Interrelating differences in structural and functional connectivity in the older adult's brain. *Human Brain Mapping* 43(18):5543–5561
- Tomasi D, Volkow ND (2012) Resting functional connectivity of language networks: characterization and reproducibility. *Mol. Psychiatry* 17:841–854
- Tremblay P, Dick A (2016) Broca and wernicke are dead, or moving past the classic model of language neurobiology. *Brain and Language* 162:60–71
- Turken A, Dronkers NF (2011) The neural architecture of the language comprehension network: converging evidence from lesion and connectivity analyses. *Frontiers in systems neuroscience* 5:1
- van den Heuvel MP, Sporns O (2013) Network hubs in the human brain. *Trends in cognitive sciences* 17(12):683–696
- Vettore M, De Marco M, Pallucca C, Bendini M, Gallucci M, Venneri A (2021) White-matter hyperintensity load and differences in resting-state network connectivity based on mild cognitive impairment subtype. *Frontiers in Aging Neuroscience* 13:737359
- Walker, G. M., Hickok, G. (2023). Are recovery of fluency and recovery of phonology antagonistic? *Brain* awad026
- Wang, Y., Chung, M., Fridriksson, J. (2022). Spectral permutation test on persistence diagrams. *Proceedings of the IEEE 47th International Conference on Acoustics, Speech and Signal Processing (ICASSP)* 1461 – 1465
- Watson CE, Gotts SJ, Martin A, Buxbaum LJ (2019) Bilateral functional connectivity at rest predicts apraxic symptoms after left hemisphere stroke. *NeuroImage: Clinical* 21:101526
- Wen, T., Hsieh, S. (2016). Network-based analysis reveals functional connectivity related to internet addiction tendency. *Frontiers in Human Neuroscience* 6
- Wertz, R. T., Deal, J. L., Robinson, A. J. (1984). Classifying the aphasias: a comparison of the boston diagnostic aphasia examination and the western aphasia battery. In: *Clinical aphasiology: Proceedings of the conference 1984* (pp. 40–47)
- Whitaker, H. (2007). Language disorders: Aphasia. In: *Encyclopedia of gerontology (second edition)* (Second Edition edn, pp. 9–16). New York: Elsevier
- Wilmskoetter J, Busby N, He X, Caciagli L, Roth R, Kristinsson S et al (2023) Dynamic network properties of the superior temporal gyrus mediate the impact of brain age gap on chronic aphasia severity. *Communications Biology* 6(1):727
- Wilson SM, Schneck SM (2020) Neuroplasticity in post-stroke aphasia: A systematic review and meta-analysis of functional imaging studies of reorganization of language processing. *Neurobiology of Language* 2(1):22–82
- Xu T, Cullen R, Mueller B, Schreiner WM, K., L. O., Schulz, S. C., Parhi, K. K. (2016) Network analysis of functional brain connectivity in borderline personality disorder using resting-state fmri. *NeuroImage: Clinical* 11:302–315
- Yang M, Li J, Li Z, Yao D, Liao W, Chen H (2017) Whole-brain functional connectome-based multivariate classification of post-stroke aphasia. *Neurocomputing* 269:199–205
- Yang M, Li Y, Li J, Li R, Pang Y, Yao D, Liao W, Chen H (2016) Altered intrinsic regional activity and interregional functional connectivity in post-stroke aphasia. *Scientific reports* 6:24803

- Yourganov G, Fridriksson J, Stark B, Rorden C (2018) Removal of artifacts from resting-state fmri data in stroke. *NeuroImage: Clinical* 17:297–305
- Yourganov G, Smith KG, Fridriksson J, Rorden C (2015) Predicting aphasia type from brain damage measured with structural mri. *Cortex* 73:203–215
- Yourganov G, Smith KG, Fridriksson J, Rorden C (2015) Predicting aphasia type from brain damage measured with structural mri. *Cortex* 73:203–215
- Yourganov G, Stark BC, Fridriksson J, Bonilha L, Rorden C (2021) Effect of stroke on contralateral functional connectivity. *Brain Connectivity* 11(7):543–552
- Zaidel D, Zaidel E, Oxbury S, Oxbury J (1995) The interpretation of sentence ambiguity in patients with unilateral focal brain surgery. *Brain and language* 51(3):458–468
- Zalesky A, Fornito A, Bullmore ET (2010) Network-based statistic: identifying differences in brain networks. *NeuroImage* 53(4):1197–1207
- Zhan Y, Yao H, Wang P, Zhou B, Zhang Z, Guo Y, Liu Y (2016) Network-based statistic show aberrant functional connectivity in alzheimer's disease. *IEEE Journal of Selected Topics in Signal Processing* 10(7):1182–1188
- Zhang B, Hua R, Qing Z, Ni L, Zhang X, Zhao H et al (2019) Abnormal brain functional connectivity coupled with hypoperfusion measured by resting-state fmri: An additional contributing factor for cognitive impairment in patients with alzheimer's disease. *Psychiatry Research: Neuroimaging* 289:18–25
- Zhu D, Chang J, Freeman S, Tan Z, Xiao J, Gao Y, Kong J (2014) Changes of functional connectivity in the left frontoparietal network following aphasic stroke. *Frontiers in behavioral neuroscience* 8:167
- Zingeser LB, Berndt RS (1990) Retrieval of nouns and verbs in agrammatism and anomia. *Brain and language* 39(1):14–32

Publisher's Note Springer Nature remains neutral with regard to jurisdictional claims in published maps and institutional affiliations.

Springer Nature or its licensor (e.g. a society or other partner) holds exclusive rights to this article under a publishing agreement with the author(s) or other rightsholder(s); author self-archiving of the accepted manuscript version of this article is solely governed by the terms of such publishing agreement and applicable law.